Journal of Solid State Chemistry 182 (2009) 2269–2273

Contents lists available at ScienceDirect

Journal of Solid State Chemistry

journal homepage: www.elsevier.com/locate/jssc

Self-powdering and nonlinear optical domain structures in ferroelastic β'-$Gd_2(MoO_4)_3$ crystals formed in glass

Y. Tsukada, T. Honma, T. Komatsu *

Department of Materials Science and Technology, Nagaoka University of Technology, 1603-1 Kamitomioka-cho, Nagaoka 940-2188, Japan

ARTICLE INFO

Article history:
Received 23 March 2009
Received in revised form
2 June 2009
Accepted 6 June 2009
Available online 12 June 2009

PACS:
78.20.−e
78.30.−j
81.05.−t
81.05.Kf

Keywords:
β'-$Gd_2(MoO_4)_3$
Ferroelasticity
Domain structure
Second harmonic generation
Crystallization
Glass

ABSTRACT

Ferroelastic β'-$Gd_2(MoO_4)_3$, (GMO), crystals are formed through the crystallization of $21.25Gd_2O_3$–$63.75MoO_3$–$15B_2O_3$ glass (mol%), and two scientific curious phenomena are observed. (1) GMO crystals formed in the crystallization break into small pieces with a triangular prism or pyramid shape having a length of 50–500 μm spontaneously during the crystallizations in the inside of an electric furnace, not during the cooling in air after the crystallization. This phenomenon is called "self-powdering phenomenon during crystallization" in this paper. (2) Each self-powdered GMO crystal grain shows a periodic domain structure with different refractive indices, and a spatially periodic second harmonic generation (SHG) depending on the domain structure is observed. It is proposed from polarized micro-Raman scattering spectra and the azimuthal dependence of second harmonic intensities that GMO crystals are oriented in each crystal grain and the orientation of $(MoO_4)^{2-}$ tetrahedra in GMO crystals changes periodically due to spontaneous strains in ferroelastic GMO crystals.

1. Introduction

Acentric gadorinium molybdate, β'-$Gd_2(MoO_4)_3$ (designated here as GMO), is a well-known unique crystal possessing both ferroelectricity and ferroelasticity [1–3], and there have been many reports on the phase transition behavior, structure, and optical properties of GMO crystals [4–8]. As a feature of ferroelasticity, GMO crystal has a domain structure, in which the direction of spontaneous polarizations or spontaneous strains (deformations) changes depending on the domain. It is of interest to design GMO crystals on substrates such as glasses for various device applications.

On the other hand, crystallization of glass is a method for the fabrication of transparent and dense condensed materials with desired shapes, nanostructures and highly oriented crystals, and a crystallization technique has been applied to various glass systems in order to design functional crystals with high performances such as second harmonic generation (SHG) or ferroelectricity [9–19]. Recently, we developed RE_2O_3–MoO_3–B_2O_3 glasses (RE: Sm, Gd, Dy) giving the crystallization of β'-$RE_2(MoO_4)_3$, and, furthermore, succeeded in patterning lines consisting of β'-$RE_2(MoO_4)_3$ crystals using a laser-induced crystallization technique [20–23]. Although many crystallized glasses consisting of functional crystals have been studied so far, the report on the synthesis of ferroelastic crystals in glasses is scarce. It is, therefore, of interest and importance to clarify the crystallization behavior of ferroelastic β'-$RE_2(MoO_4)_3$ crystals in glasses and to characterize their micro-structures and optical properties from the scientific and device application points of view.

The purpose of this study is to examine the crystallization behavior of Gd_2O_3–MoO_3–B_2O_3 glasses more in detail and to characterize nonlinear optical properties (i.e., SHG) of GMO crystals formed by the crystallization. In this study, we found two curious phenomena. The first one is that GMO crystals formed in the crystallization break into small pieces spontaneously during the crystallizations in the inside of an electric furnace, not during the cooling in air after the crystallization. We propose to call this "self-powdering phenomenon during crystallization" in this paper. The second one is that each self-powdered GMO crystal grain shows a periodic domain structure giving a periodic

* Corresponding author.
E-mail address: komatsu@mst.nagaokaut.ac.jp (T. Komatsu).

0022-4596/$ - see front matter © 2009 Elsevier Inc. All rights reserved.
doi:10.1016/j.jssc.2009.06.009

refractive index change. The present study, therefore, reports a unique crystallization behavior and characterizations of ferroelastic β'-$Gd_2(MoO_4)_3$ crystals formed in glasses.

2. Experimental

Considering previous reports [20–23], a glass with the composition of $21.25Gd_2O_3$–$63.75MoO_3$–$15B_2O_3$ (mol%) was prepared using a conventional melt quenching technique. Commercial powders of reagent grade Gd_2O_3, MoO_3, and B_2O_3 were melted in a platinum crucible at 1100 °C for 30 min in an electric furnace. The melts were poured onto an iron plate and pressed to a thickness of ~1.5 mm by another iron plate. Glass transition, T_g, crystallization onset, T_x, and crystallization peak, T_p, temperatures were determined using differential thermal analyses (DTA) at a heating rate of 10 K/min.

The glasses with a plate shape were heat treated at some temperatures, and the crystalline phase present in the crystallized samples was identified by X-ray diffraction (XRD) analyses (Cu$K\alpha$ radiation) at room temperature. Polarized micro-Raman scattering spectra at room temperature for the precursor glass and crystallized samples were measured with a laser microscope (Tokyo Instruments Co., Nanofinder) operated at Ar^+ laser (wavelength: $\lambda = 488$ nm). In our micro-Raman apparatus, the data below ~250 cm^{-1} cannot be measured due to the use of an edge filter. SHGs of crystallized samples were examined by measuring the intensity of second harmonic (SH) light ($\lambda = 532$ nm) for the incident light of a Q-switched Nd: yttrium aluminum garnet (YAG) laser with $\lambda = 1064$ nm [24].

3. Results and discussion

3.1. Self-powdering phenomenon of crystallized glasses

The DTA pattern of the as-quenched sample of $21.25Gd_2O_3$–$63.75MoO_3$–$15B_2O_3$ glass (designated here as GMB glass) is shown in Fig. 1. An endothermic peak due to the glass transition and an exothermic peak due to the crystallization are clearly observed, and the values of $T_g = 540$ °C, $T_x = 571$ °C, and $T_p = 585$ °C are obtained. The optical photographs at room temperature for the samples obtained by heat treatments at temperatures of around T_g, T_x and T_p for 2 h in air are shown in Fig. 2. The sample heat-treated at $T_g = 540$ °C remained optical transparent and in the original shape. On the other hand, the samples heat-treated at around crystallization onset and peak temperatures are becoming powders. It was confirmed experimentally that the powdering of the samples is taking place during the crystallization in the inside of an electric furnace, not during the cooling process after heat treatments. That is, the heat-treated glasses themselves break into small pieces during the crystallization at high temperatures of 570 and 590 °C. We propose to call this phenomenon "self-powdering phenomenon during crystallization" in this paper. The optical photographs at room temperature for the powders obtained by heat treatments at 570 and 590 °C are shown in Fig. 3. It is seen that small pieces having sharp edges and a triangular prism or pyramid shape. The length was found to be 300–500 μm for the particles obtained at a

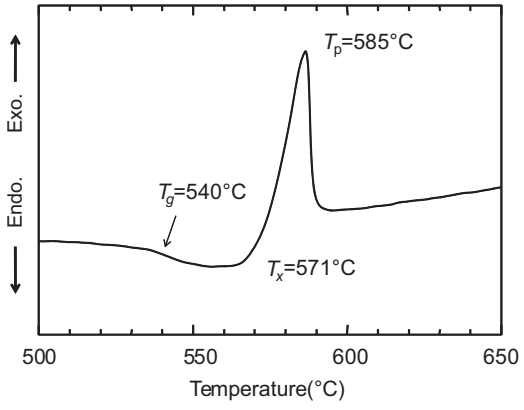

Fig. 1. DTA pattern at room temperature for the melt-quenched sample with the composition of $21.25Gd_2O_3$–$63.75MoO_3$–$15B_2O_3$. Heating rate was 10 K/min.

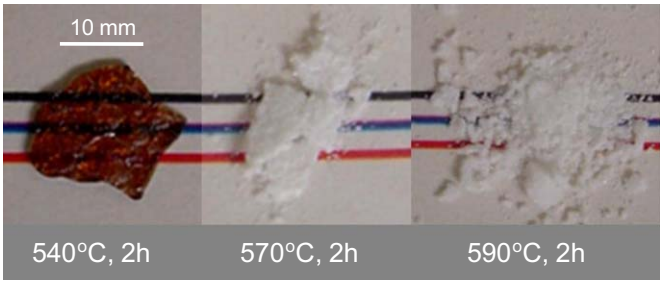

Fig. 2. Optical photographs at room temperature for the samples obtained by heat treatments of $21.25Gd_2O_3$–$63.75MoO_3$–$15B_2O_3$ glass at 540, 570, and 590 °C for 2 h in an electric furnace in air.

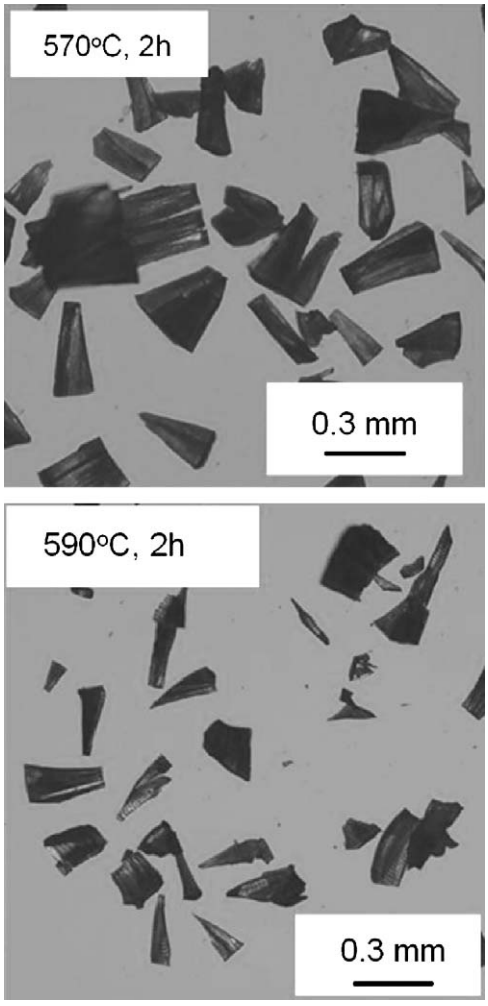

Fig. 3. Optical photographs at room temperature for the samples obtained by heat treatments of the glass at 570 and 590 °C for 2 h in air in an electric furnace.

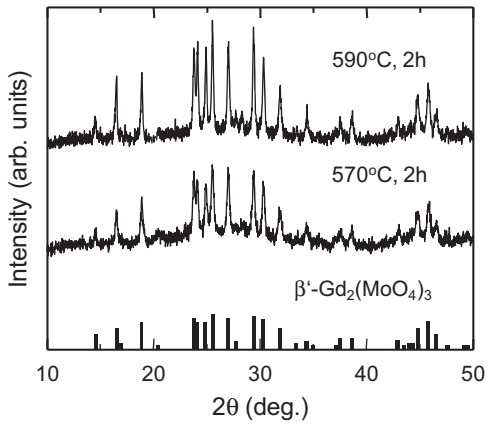

Fig. 4. Powder XRD patterns at room temperature for the crystallized samples obtained by heat treatments of the glass at 540, 570, and 590 °C for 2 h in an electric furnace in air. The peaks are assigned to β'-$Gd_2(MoO_4)_3$ crystals.

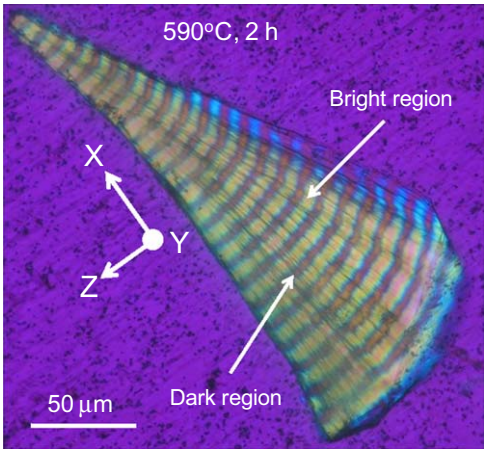

Fig. 5. Polarized optical photograph for a particle (piece) obtained by a heat treatment of the glass at 590 °C for 2 h in an electric furnace in air.

heat treatment of 570 °C, 200–400 μm for the particles obtained at a heat treatment of 590 °C, and 50–200 μm for the particles obtained at a heat treatment of 640 °C, indicating that the size of particles tends to decrease with increasing heat treatment temperature and thus depends on the heat treatment condition.

The XRD patterns at room temperature for the powders obtained by heat treatments at 570 and 590 °C for 2 h are shown in Fig. 4. The peaks are assigned to β'-$Gd_2(MoO_4)_3$ crystals (JCPDS: No. 01-070-1397 and Ref. [22]). The phase diagram and the structure of rare-earth molybdates, $RE_2(MoO_4)_3$, where RE = Pr, Nd, Sm, Eu, Gd, Tb, Dy, have been studied extensively [4,5, 25–28]. The thermodynamically stable phase in the temperatures below 800–990 °C is the α-$RE_2(MoO_4)_3$ phase with a monoclinic structure ($C2/c$). In the temperature range of $1000 < T < 1200$ °C, the β-$RE_2(MoO_4)_3$ phase with a tetragonal structure ($P42_1m$) is stable. The β phase (paraelectric) transforms to the β'-$RE_2(MoO_4)_3$ phase (ferroelectric) with an orthorhombic structure ($Pba2$) below Curie temperature [28]. It should be emphasized that the crystalline phase through the crystallization of GMB glass is the ferroelectric β'-$Gd_2(MoO_4)_3$ phase, but not the paraelectric α-$Gd_2(MoO_4)_3$ phase.

The Curie temperature T_c of the β'-$Gd_2(MoO_4)_3$ phase is 163 °C [2], and thus the heat treatment temperatures of 570 and 590 °C taking place in the self-powdering phenomenon are much higher compared with T_c = 163 °C. That is, GMO crystals formed during the crystallization at 570 and 590 °C are not ferroelastic at the temperatures of 570 and 590 °C, but paraelastic. In other words, the driving force inducing the breaking into small pieces is not a spontaneous strain arising from the ferroelasticity. It has been reported that GMO single crystals exhibit perfect cleavages along the (100) and (110) planes [2,29]. It has been reported that the thermal expansion coefficients (α) of GMO crystal at room temperature are $\alpha_a = 18.3 \times 10^{-6}$/K for the a-axis, $\alpha_b = 16.7 \times 10^{-6}$/K for the b-axis, and $\alpha_c = -4.7 \times 10^{-6}$/K for the c-axis [30]. It is noted that even at the temperature of 200 °C (higher than T_c = 163 °C), the c-axis shows the negative values of $\alpha_c = -4.9 \times 10^{-6}$/K. The presence of the positive and negative thermal expansions would induce strains within GMO crystal itself together with the increase (growth) in GMO crystal's size. That is, the thermal expansion feature in GMO crystals might be one of the reasons for the self-powdering phenomenon observed in the present study. It is desired to study on the self-powdering phenomenon of other β'-$RE_2(MoO_4)_3$ crystals during the crystallization in RE_2O_3–MoO_3–B_2O_3 glasses.

The polarization optical photograph for a crystal grain (piece) obtained by a heat treatment at 590 °C for 2 h is shown in Fig. 5. The color is not uniform over the whole region of the grain. The bright and dark regions are formed periodically, meaning the formation of the domain structure with a periodic refractive index change, i.e., the periodic arrangement of the high refractive index region (i.e., the bright region) and the low refractive index region (i.e., the dark region). This kind of the periodic color change is observed in other pieces as a common feature. As can be seen in Fig. 5, the length of the bright region is 4.5–7 μm and that of the dark region is 3.5–5 μm. In ferroelectric crystals, a periodic domain structure having oppositely polarized ferroelectric domains is created by using a periodic poling technique. Yuan et al. [31] fabricated GMO single crystals (500 μm thick slices) with a periodic domain structure (period: 5.54 μm) and observed clear SHGs. At least, the results shown in Fig. 5 indicate that domains with different polarized directions are periodically created in each GMO crystal grain formed in the crystallization of $21.25Gd_2O_3$–$63.75MoO_3$–$15B_2O_3$ glass.

The polarized micro-Raman scattering spectra at room temperature for the bright and dark regions in a crystal piece obtained by a heat treatment at 590 °C for 2 h are shown in Figs. 6 and 7, respectively, in which the spectra for the configurations of $y(xx)y$ and $y(zz)y$ are measured and the definition of the configuration for the region is indicated in Fig. 5. Several sharp peaks are observed in both regions, indicating that both regions are crystallized. And, furthermore, the peaks are assigned to the GMO crystalline phase [20–23,32–34], indicating that both regions consist of the same crystalline phase of GMO. In the structure of the acentric orthorhombic β'-$RE_2(MoO_4)_3$ phase, REO_7 polyhedra (monocapped trigonal prisms) and MoO_4 tetrahedra are present and they are linked together via common corners [35]. It is known that three different types of $(MoO_4)^{2-}$ tetrahedra having different mean distances of Mo–O bonds are present in GMO crystals, i.e., types I, II, and III, and three crystallographically independent $(MoO_4)^{2-}$ tetrahedra form successive layers along the c-axis [3,32–34]. Each $(MoO_4)^{2-}$ tetrahedron is discrete, and each oxygen atom in $(MoO_4)^{2-}$ is bonded only to one Mo atom, in addition to either one or two Gd atoms [3]. All peaks appeared in the Raman scattering spectra (Figs. 6 and 7) are assigned to the bending or stretching vibrations in Mo–O bonds in $(MoO_4)^{2-}$ tetrahedra [32–34]. That is, the peaks at ~323 and 379–382 cm^{-1} are assigned to the bending modes of Mo–O bonds, the peaks at 741–748 and 846–852 cm^{-1} are due to the antisymmetric Mo–O stretching vibrations in type II or III, the peak at 819–829 cm^{-1} is due to the antisymmetric Mo–O stretching vibrations in type I, the peaks at 944 and 956–958 cm^{-1} are assigned to the symmetric Mo–O stretching vibrations in types I and II or III, respectively.

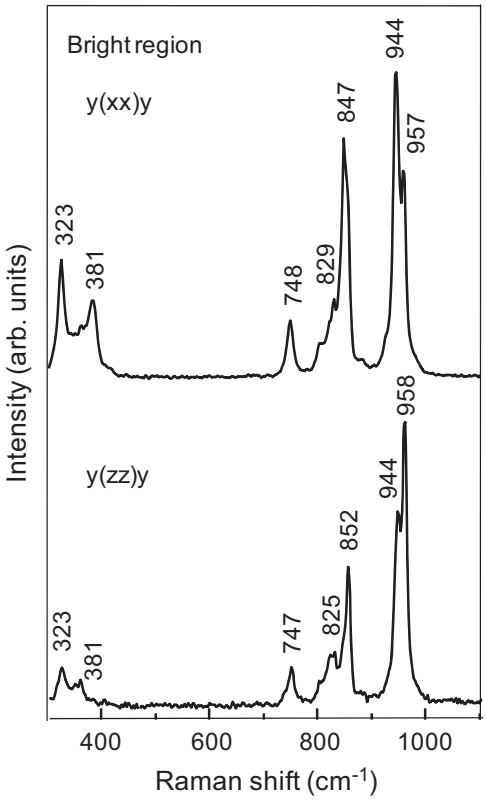

Fig. 6. Polarized micro-Raman scattering spectra for the bright region (Fig. 5) of a particle (piece) obtained by a heat treatment of the glass at 590 °C for 2 h in an electric furnace in air.

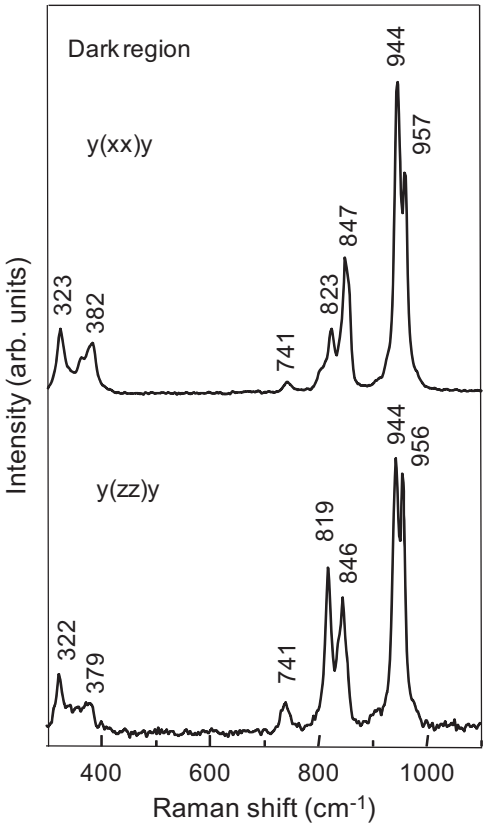

Fig. 7. Polarized micro-Raman scattering spectra for the dark region (Fig. 5) of a particle (piece) obtained by a heat treatment of the glass at 590 °C for 2 h in an electric furnace in air.

Considering the structure of GMO crystal, the difference in the polarized micro-Raman scattering spectra (Figs. 6 and 7) suggests that GMO crystals in the bright and dark regions might be oriented. That is, the anisotropic orientation of three different types of $(MoO_4)^{2-}$ tetrahedra might be induced depending on the domain structure.

3.2. Periodic second harmonic generations

The photograph for the SHG microscope observation for a self-powdered crystal grain consisting of GMO crystals is shown in Fig. 8. The SH light is detected from the grain, but it should be pointed out that the intensity of SH light changes periodically depending on the position of the specimen. That is, SHGs are clearly observed in the bright region appeared in the polarized optical photograph, but the dark region gives extremely weak SH intensities. The appearance of periodic SHGs is extremely curious, because both regions consist of GMO crystals. However, as shown in the polarized micro-Raman scattering spectra (Figs. 6 and 7), three different types of $(MoO_4)^{2-}$ tetrahedra in GMO crystals have been suggested to be oriented in each domain. Kim et al. [36] examined the characteristics of SHGs in GMO crystals grown by the Czochralski method and reported the value of $d_{eff} = 1.2$ pm/V as the effective second order non-linear optical coefficient. Bonneville and Auzel [37] proposed that the major part of non-linear optical properties in GMO crystals is due to the orientation of MoO4 tetrahedra and the Mo–O bond hyperpolarizability.

The azimuthal dependence of SH intensities for a crystal grain (Fig. 5) is shown in Fig. 9. The notations of H–H and H–V mean that the polarized electric field of the incident laser is parallel or perpendicular to the electric field of SH light in the measurements, respectively. Furthermore, the rotation angles of

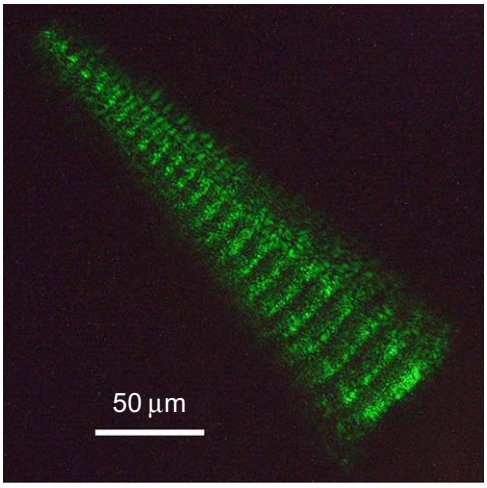

Fig. 8. Photograph for the SHG microscope observation for a particle (piece) obtained by a heat treatment of the glass at 590 °C for 2 h in an electric furnace in air. The bright regions observed in the polarized optical photograph (Fig. 5) give clear SH light.

0° and 180° in the experiments correspond to the configuration that the polarized electric field of the incident laser is parallel to the long axis direction in a grain, i.e., *X*-direction in Fig. 5, and the rotation angles of 90° and 270° mean that the polarized electric field of the incident laser is perpendicular to the line growth direction, i.e., *Z*-direction in Fig. 5. As can be seen in Fig. 9, the SH intensities change depending on the rotation angle. In the H–H configuration, four clear peaks are observed at the angles of $\theta_1 \sim 48°$, $\theta_2 \sim 130°$, $\theta_3 \sim 232°$, and $\theta_4 \sim 315°$. It should be pointed out

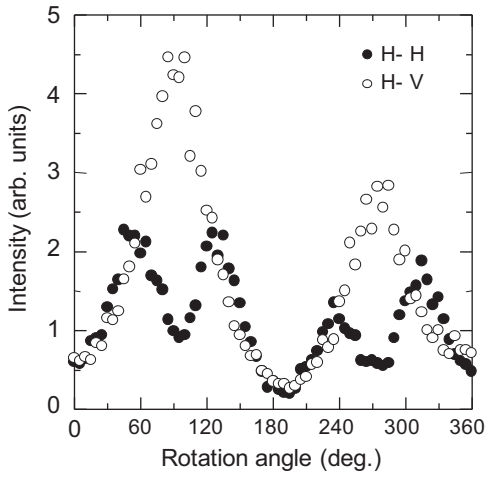

Fig. 9. Azimuthal dependence of the second harmonic intensities for a crystal grain. The notations of H–H and H–V mean that the polarized electric field of the incident laser is parallel or perpendicular to the electric field of SH light in the measurements, respectively.

that the separations among these angles are 82–102°, e.g., $\Delta\theta = \theta_2 - \theta_1 = 82°$. The separation between θ_1 and θ_3 is ~184° and that between θ_2 and θ_4 is ~185°. On the other hand, in the H–V configuration, two peaks are observed at ~90° and ~270°. These data suggest again that GMO crystals in each grain are oriented. Aizu et al. [2] reported that the piezoelectric moduli of d_{36} and d_{312} in ferroelastic GMO single crystals are referred to the system of the coordinate axes resulting from the rotation of the *a*- and *b*-axes about the *c*-axis through 45°. Therefore, if the long axis in the crystal grain corresponds to the *c*-axis direction of GMO, it is expected that strong SHGs would be observed at the angle of 135°, which is a 45° deviation from the long axis direction. Indeed, as shown in Fig. 9, strong SHGs are observed at such angles.

Very recently, we have succeeded in the patterning of ferroelastic β'-$(Sm,Gd)_2(MoO_4)_3$, (SGMO), crystal lines on the surface of Sm_2O_3–Gd_2O_3–MoO_3–B_2O_3 glasses by continuous-wave Yb:YVO_4 laser irradiations (wavelength: 1080 nm, power: 1.2 W, scanning speed: 5 μm/s) and found that the crystal lines show a self-organized periodic domain structure with a periodic refractive index change [23]. Furthermore, we also found that the intensity of SH light changes periodically depending on the domain structure. It has been proposed from the azimuthal dependence of SH intensities that the orientation of $(MoO_4)^{2-}$ tetrahedra in SGMO crystals changes gradually and periodically along the crystal line growth direction due to spontaneous strains in SGMO crystals [23]. It should be emphasized that the periodic domain structure and SH intensity (Figs. 5 and 8) observed in the crystal grains are similar to those in the crystal lines. That is, it is concluded that the formation of the periodic domain structure observed in GMO crystal specimens (obtained by a usual crystallization in an electric furnace) and β'-$(Sm,Gd)_2(MoO_4)_3$ crystal lines (patterned by laser irradiations) might be intrinsic for ferroelastic β'-$RE_2(MoO_4)_3$ crystals. The most peculiar feature in β'-$RE_2(MoO_4)_3$ crystals is the ferroelectric–ferroelastic transition, i.e., spontaneous strains are created in the crystals. At this moment, it is considered that spontaneous strains would create periodic orientation changes in $(MoO_4)^{2-}$ tetrahedra in β'-$Gd_2(MoO_4)_3$ crystals and induce periodic SHGs depending on the domain structure. Further studies, in particular on the crystallization mechanism of GMO crystals in Gd_2O_3–MoO_3–B_2O_3 glasses, would be necessary to clarify the origin of self-powdering phenomenon and domain structure.

4. Conclusions

The crystallization behavior and micro-structure of ferroelastic β'-$Gd_2(MoO_4)_3$, (GMO), crystals in $21.25Gd_2O_3$–$63.75MoO_3$–$15B_2O_3$ glass (mol%) were examined. It was found that GMO crystals formed in the crystallization broke into small pieces spontaneously during the crystallization in the inside of an electric furnace, not during the cooling in air after the crystallization. It was also found that each self-powdered GMO crystal showed a periodic domain structure with different refractive indices. The spatially periodic second harmonic generation depending on the domain structure was observed in each crystal particle and was discussed from the point of the orientation of different types of $(MoO_4)^{2-}$ tetrahedra in GMO crystals.

Acknowledgment

This work was supported by the Grant-in-Aid for Scientific Research from the Ministry of Education, Science, Sports, Culture and Technology, Japan.

References

[1] H.J. Borchardt, P.E. Bierstedt, Appl. Phys. Lett. 8 (1966) 50.
[2] K. Aizu, A. Kumada, H. Yumoto, S. Ashida, J. Phys. Soc. Jpn. 27 (1969) 511.
[3] E.T. Keve, S.C. Abrahams, J.L. Bernstein, J. Chem. Phys. 54 (1971) 3185.
[4] K. Nassau, J.W. Shiever, E.T. Keve, J. Solid State Chem. 3 (1971) 411.
[5] W. Jeitschko, Acta Cryst. B 28 (1972) 60.
[6] A. Kumada, Ferroelectrics 3 (1972) 115.
[7] A.N. Alexeyev, D.V. Roshchupkin, Appl. Phys. Lett. 68 (1996) 159.
[8] H. Nishioka, W. Odajima, M. Tateno, K. Ueda, A.A. Kaminskii, A.V. Butashin, S.N. Bagayev, A.A. Pavlyuk, Appl. Phys. Lett. 70 (1997) 1366.
[9] G.H. Beall, L.R. Pinckney, J. Am. Ceram. Soc. 82 (1999) 5.
[10] R. Sakai, Y. Benino, T. Komatsu, Appl. Phys. Lett. 77 (2000) 2118.
[11] N.S. Prasad, K.B.R. Varma, Y. Takahashi, Y. Benino, T. Fujiwara, T. Komatsu, J. Solid State Chem. 173 (2003) 209.
[12] H. Jain, Ferroelectrics 306 (2004) 111.
[13] P. Gupta, H. Jain, D.B. Williams, J. Toulouse, I. Veltchev, Opt. Mater. 29 (2006) 355.
[14] I. Enomoto, Y. Benino, T. Fujiwara, T. Komatsu, J. Solid State Chem. 179 (2006) 1821.
[15] D. Vouagner, C. Coussa, C. Martinet, H. Hugueney, B. Champagnon, V. Califano, V. Sigaev, J. Non-Cryst. Solids 353 (2007) 1910.
[16] M.J. Davis, P. Vullo, I. Mitra, P. Blaum, K.A. Gudgel, N.J. Donnelly, C.A. Randall, J. Am. Ceram. Soc. 91 (2008) 2878.
[17] R.C.C. Figuera, M.P.F. Graca, L.C. Costa, M.A. Valente, J. Non-Cryst. Solids 354 (2008) 5162.
[18] Y. Hane, T. Komatsu, Y. Benino, T. Fujiwara, J. Appl. Phys. 103 (2008) 063512.
[19] N. Maruyama, T. Honma, T. Komatsu, J. Chem. Phys. 128 (2008) 184706.
[20] M. Abe, Y. Benino, T. Fujiwara, T. Komatsu, R. Sato, J. Appl. Phys. 97 (2005) 123516.
[21] R. Nakajima, M. Abe, Y. Benino, T. Fujiwara, H.G. Kim, T. Komatsu, J. Non-Cryst. Solids 353 (2007) 85.
[22] R. Nakajima, T. Honma, Y. Benino, T. Komatsu, J. Ceram. Soc. Jpn. 115 (2007) 582.
[23] Y. Tsukada, T. Honma, T. Komatsu, Appl. Phys. Lett. 94 (2009) 059901.
[24] T. Fujiwara, T. Sawada, Y. Benino, T. Komatsu, M. Takahashi, T. Yoko, J. Nishii, Jpn. J. Appl. Phys. 42 (2003) 7326.
[25] K. Nassau, H.J. Levinstein, G.M. Loiacono, J. Phys. Chem. Solids 26 (1965) 1805.
[26] K. Nassau, P.B. Jamieson, J.W. Shiever, J. Phys. Chem. Solids 30 (1969) 1225.
[27] P.A. Fleury, Solid State Commun 8 (1970) 601.
[28] V. Dimitriev, V. Sinitsyn, R. Dilanian, D. Machon, A. Kuznetsov, E. Ponyatovsky, G. Lucazeau, H.P. Weber, J. Phys. Chem. Solids 64 (2003) 307.
[29] P. Panfilov, Y.L. Gagarin, V.Ya. Shur, J. Mater. Sci. 34 (1999) 241.
[30] J. Kobayashi, Y. Sato, T. Nakamura, Phys. Stat. Sol. (A) 14 (1972) 259.
[31] Q. Yuan, T. Reh, G. Luo, S. Pan, J. Xu, Y. Zhu, S. Zhu, J. Cryst. Growth 243 (2002) 185.
[32] F.G. Ulman, B.J. Holden, B.N. Gauguly, J.R. Hardy, Phys. Rev. B 8 (1973) 2991.
[33] S.S. Saleem, G. Aruldhas, H.D. Bist, J. Solid State Chem. 48 (1983) 77.
[34] L. Guy, M. Denis, J. Raman Spectrosc. 37 (2006) 189.
[35] A.A. Kaminskii, V. Butashin, H.J. Eichler, D. Grebe, R. Macdonald, K. Ueda, H. Nishiguchi, W. Odajima, M. Tateno, J. Song, M. Musha, S.N. Bagaev, A.A. Pavlyuk, Opt. Mater. 7 (1997) 59.
[36] S.I. Kim, J. Kim, S.C. Kim, S.I. Yun, T.Y. Kwon, Mater. Lett. 26 (1995) 195.
[37] R. Bonneville, F.J. Auzel, J. Chem. Phys. 67 (1977) 4597.